Singular vectors, forecast errors and the pseudo-inverse

Roberto Buizza

European Centre for Medium-Range Weather Forecasts (www.ecmwf.int)

Union City, OK, 24 May 1973.

Outline

- Definition of singular vectors: brief summary.
- Singular vectors and the pseudo-inverse initial perturbation.
- Two examples from FASTEX.
- Conclusions.

Singular vector definition

Consider an N-dimensional system:

$$\frac{\partial y}{\partial t} = A(y)$$

Denote by ***z'*** a small perturbation around a time-evolving trajectory ***z***:

$$\frac{\partial z'}{\partial t} = A_l(z)z' \qquad A_l(z) = \left.\frac{\partial A(z)}{\partial z}\right|_z$$

$$\frac{\partial z}{\partial t} = A(z)$$

The time evolution of the small perturbation ***z'*** is described to a good degree of approximation by the linearized system $\boldsymbol{A_l(z)}$ defined by the trajectory. Note that the trajectory is not constant in time.

Singular vector definition (cont)

The solution of the linearized system can be written in terms of the linear propagator *L(t,0)*:

$$z'(t) = L(t,0)z'_0$$

The linear propagator is defined by the system equations and depends on the trajectory characteristics.

The E-norm of the perturbation at time ***t*** is given by:

$$\|z'(t)\|^2 = \langle z'(t); Ez'(t) \rangle = \langle L(t,0)z'_0; EL(t,0)z'_0 \rangle$$

Singular vector definition (cont)

The computation of the directions of maximum growth can be stated as 'finding the directions in the phase-space of the system characterized by the maximum ratio between the time-t and the initial norms':

$$\max_{x_0 \in \Sigma} \frac{\|x(t)\|_E^2}{\|x_0\|_{E_0}^2} = \max_{x_0 \in \Sigma} \frac{< x_0; L^* E L x_0 >}{< x_0; E_0 x_0 >}$$

The problem reduces to solving the following eigenvalue problem:

$$E_0^{-1/2} L^* E L E_0^{-1/2} v = \sigma^2 v$$

Redefinition of SVs using the SVD theorem

Given the linear propagator L(t,0), denote by

$$U = [u_1,..,u_m] \in R^{mxm} \qquad V = [v_1,..,v_n] \in R^{nxn}$$

the two orthogonal matrices that define the SVD of L:

From:

$$U^T L V = \Sigma \qquad L = U \Sigma V^T$$

it follows that:

$$L v_i = \sigma_i u_i \qquad L^T u_i = \sigma_i v_i$$

The singular values σ_i are the length of the semi-axes of the hyper-ellipsoid E defined by $L^T L$ that coincide with the left singular vectors u_i.

$$L^T L v_i = L^T \sigma_i u_i = \sigma_i^2 v_i \qquad L L^T u_i = L \sigma_i v_i = \sigma_i^2 u_i$$

Redefinition of SVs from SVD theorem (cont)

The right singular vectors v_i define the vectors that evolve into the left singular vectors.

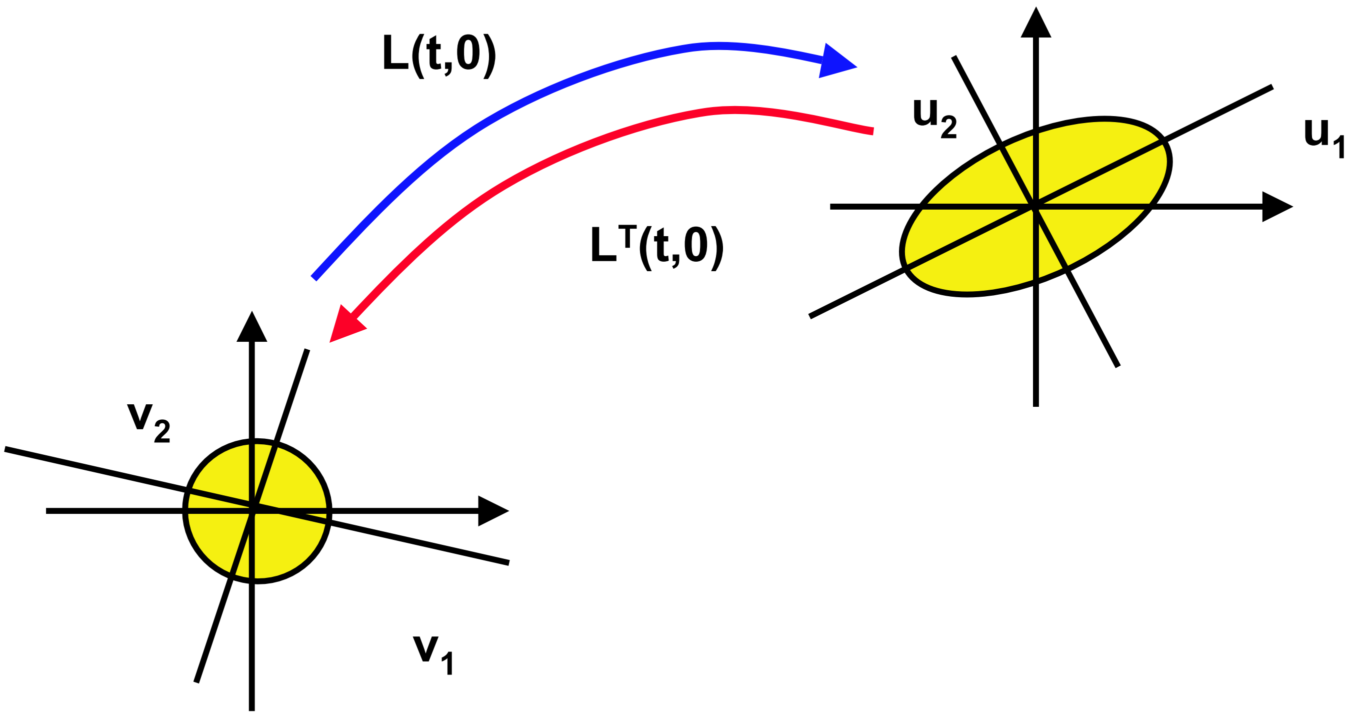

Forecast errors, SVs and pseudo-inverse

The singular vectors of the linear propagator can be used to estimate the origin of forecast errors. Denote by f(d,t) a forecast started at day d and valid for day d+t. Consider the forecast f(d,t) and the corresponding verifying analysis f(d+t,0). The forecast error is given by:

$$e(d,t) = f(d,t) - f(d+t,0)$$

Consider the linear propagator L(d+t,d) and the singular vectors growing between day d and d+t:

$$U^T L V = \Sigma$$

$$L(d+t,d)v_i = \sigma_i u_i$$

Forecast errors, SVs and pseudo-inverse (cont)

Problem: find the smallest initial perturbation e(d,0) that evolves into the forecast error e(d,t). This can be approached in the following two ways:

1. **Pseudo-inverse** field. Look for **ε(d,0)** such that:

$$L(d+t,d)\varepsilon(d,0)=e(d,t)$$

i.e.:

$$\varepsilon(d,0)=[L(d+t,d)]^{-1}e(d,t)$$

2. **Sensitivity** field. Look for **γ(d,0)** such that its time evolution has a maximum projection onto e(d,t):

$$\max_{\gamma(d,0)} < L(d+t,d)\gamma(d,0);e(d,t) >$$

i.e.:

$$\gamma(d,0)=\beta\cdot[L(d+t,t)]^{T}e(d,t)$$

where β is a constant.

Forecast errors, SVs and pseudo-inverse (cont)

In approach 1 the **inverse** and in approach 2 the **adjoint** of the linear propagator are to be computed. This is not easy for complex systems with a very large number of degrees of freedom $M_{sys}>>1$.

For such systems, iterative procedures allow to compute the leading N singular vectors, with $N<<M_{sys}$, and since the leading singular vectors defines the phase-space directions along which perturbation growth is maximized, it is thought that they can be used to construct valid approximations of the inverse and the adjoint of the linear propagator:

$$\tilde{L} = U_N \Sigma_N V_N^T \qquad \tilde{L}^{-1} = V_N \Sigma_N^{-1} U_N^T \qquad \tilde{L}^T = V_N \Sigma_N U_N^T$$

These approximations coincide with the inverse and the adjoint in the unstable sub-space of the phase-space of the system spanned by the leading N singular vectors.

Forecast errors and singular vectors (cont)

Then:

$$\tilde{\varepsilon}(d,0) = [\tilde{L}(d+t,d)]^{-1} e(d,t) = V_N \Sigma_N^{-1} U_N^T e(d,t)$$

$$\tilde{\gamma}(d,0) = \beta \cdot [\tilde{L}(d+t,t)]^T e(d,t) = \beta \cdot V_N \Sigma_N U_N^T e(d,t)$$

More explicitly:

$$\tilde{\varepsilon}(d,0) = \sum_{j=1,N} \frac{1}{\sigma_j} < u_j ; e(d,t) > v_j$$

$$\tilde{\gamma}(d,0) = \beta \cdot \sum_{j=1,N} \sigma_j < u_j ; e(d,t) > v_j$$

The first field is called the **pseudo-inverse** field and the second field is called the **sensitivity** field.

Forecast errors and singular vectors (cont)

The two fields differ by the weighting of the singular vectors used in the projection:

$$\tilde{\gamma}(d,0) = \beta \cdot V_N \Sigma_N^2 V_N^T \tilde{\varepsilon}(d,0)$$

By applying the approximate linear propagator it can be verified that:

$$\tilde{\varepsilon}(d,t) = \tilde{L}(d+t,d)\tilde{\varepsilon}(d,0) = \sum_{j=1,N} \frac{1}{\sigma_j} < u_j; e(d,t) > \tilde{L} v_j = \sum_{j=1,N} < u_j; e(d,t) > u_j$$

$$\tilde{\gamma}(d,t) = \tilde{L}(d+t,d)\tilde{\gamma}(d,0) = \beta \cdot \sum_{j=1,N} \sigma_j < u_j; e(d,t) > \tilde{L} v_j =$$

$$= \beta \cdot \sum_{j=1,N} \sigma_j^2 < u_j; e(d,t) > u_j$$

Example: pseudo-inverse initial perturbation for 2 cases

Problem. Investigate the role of the leading singular vectors in describing the growth of the forecast error during the first 2 days of forecast, in particular for the area A={40:60N;20-0W}. Identify also the region of possible origin of forecast error.

Solution. Compute the singular vectors growing during 48-h with maximum final time norm inside the area A. Project the 48-h forecast error onto the leading (in this case 4) singular vectors; compare the projected and the full forecast error. Determine the initial time pseudo-inverse initial perturbation.

Examples refer to two cases of February and March 1996, with singular vectors computed with a T63L19 resolution (*Buizza & Montani*, 1999).

Ex: analysis (Z500) at initial and 48-h forecast times

7-9 Feb 1996

10-12 Mar 1996

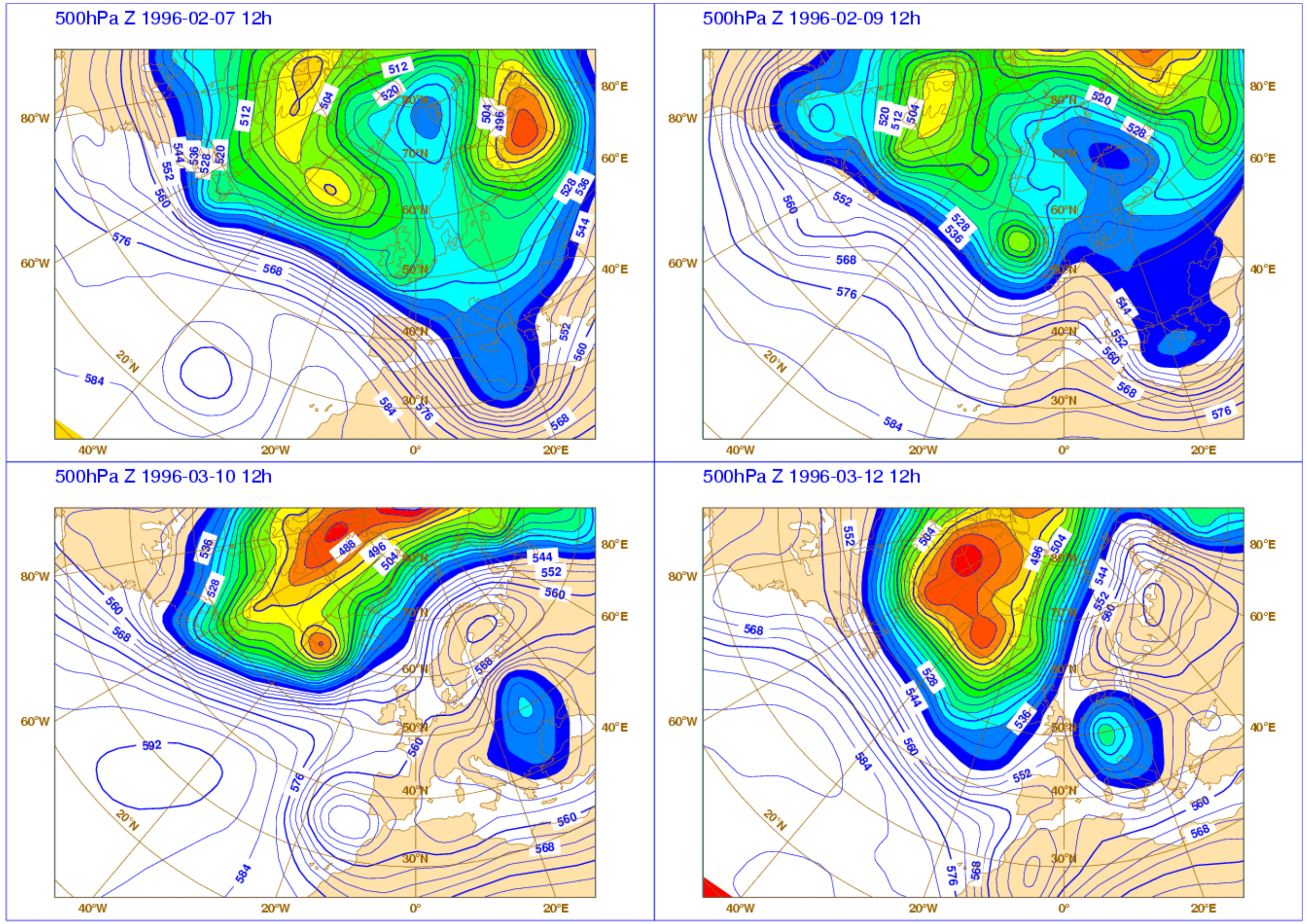

Ex1: pseudo-inv and forecast error for Feb 1996 case

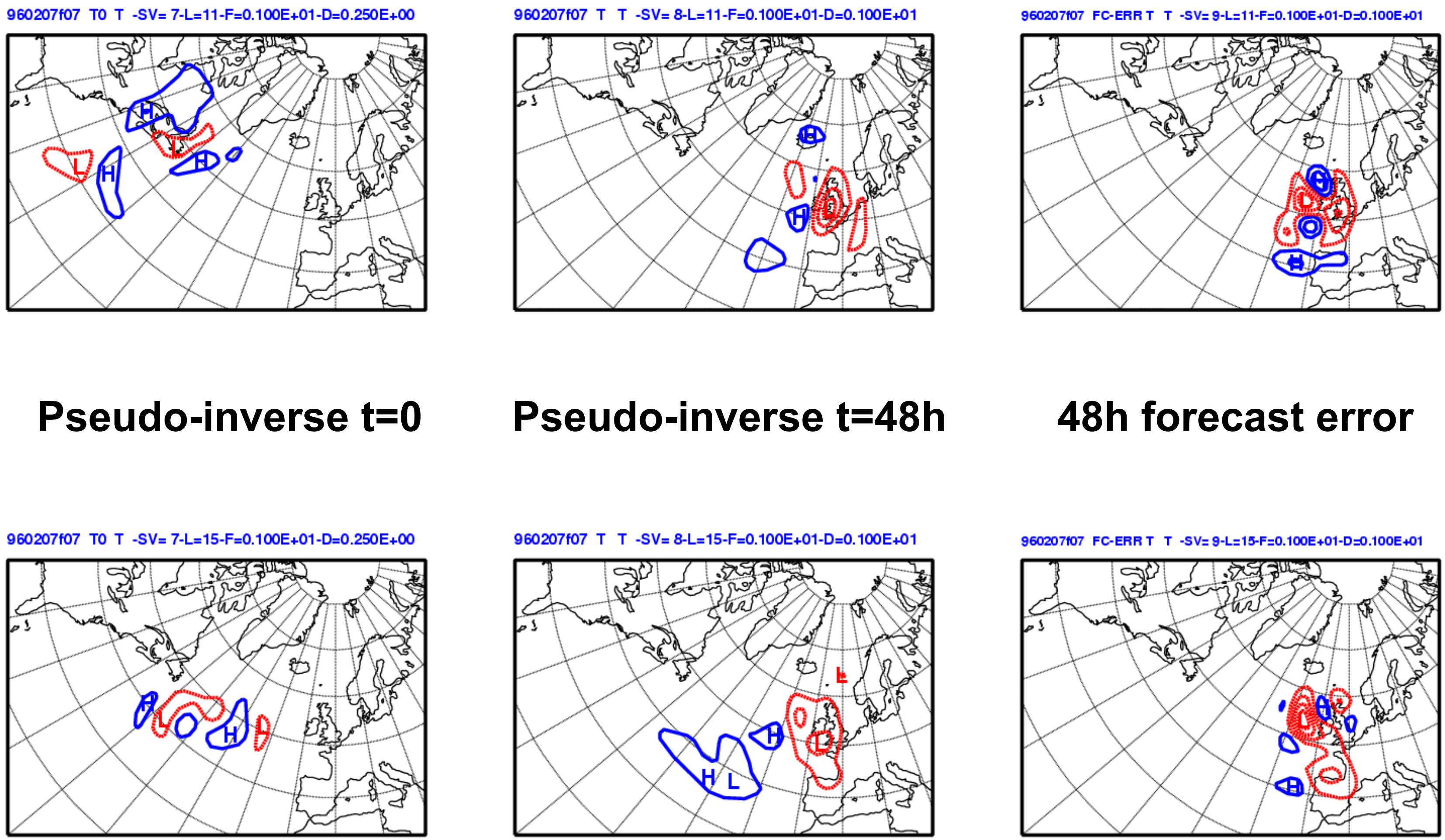

Lev=11

(~500hPa)

Lev=15

(~700hPa)

Ex2: pseudo-inv and forecast error for Mar 1996 case

Lev=11

(~500hPa)

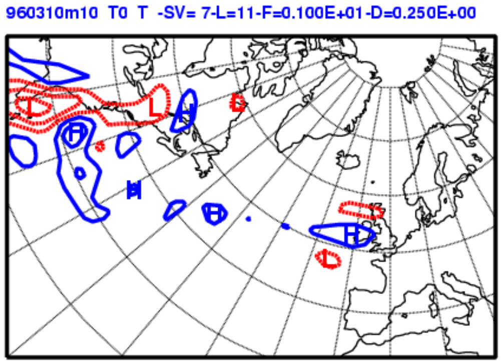

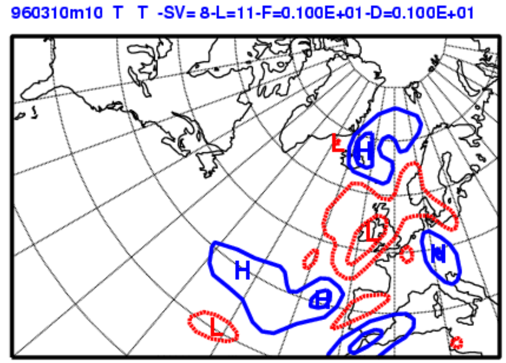

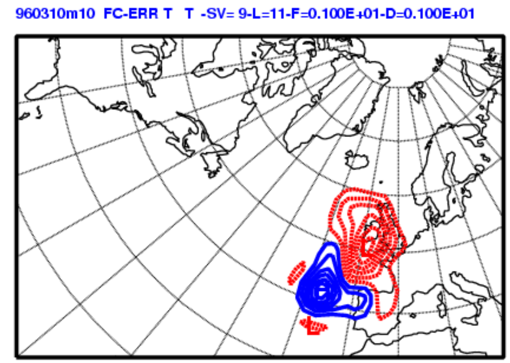

Pseudo-inverse t=0 **Pseudo-inverse t=48h** **48h forecast error**

Lev=15

(~700hPa)

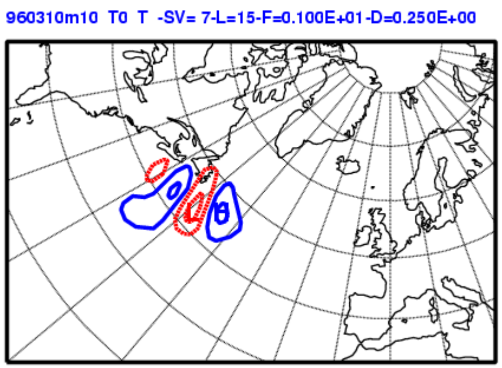

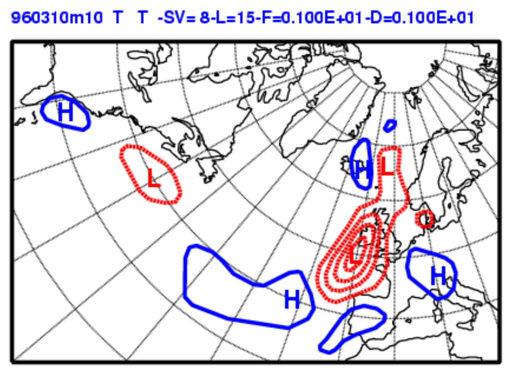

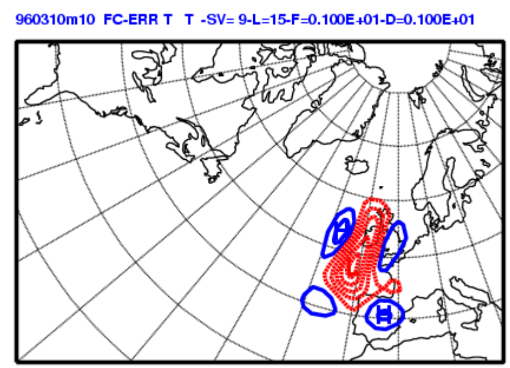

Ex1-2: norm of projected and complete forecast error

The following table lists the (total energy) norm of the 48-h forecast error inside the region A={40:60N;20-0W}, and the norm of the projection of the forecast error on the leading 4 singular vectors with maximum final norm inside A. The ratio of the two norms gives an indication of the importance of the directions defined by the leading singular vectors in capturing error growth.

	||48h fc error ||	|| pseudo-inv t=48h ||	ratio
7-Feb-96	143	85	59.4%
10-Mar-96	249	140	56.2%

Ex1-2: total energy vertical distributions and spectra

To investigate in more details the relationship between singular vectors and forecast error growth, it is of interest to compare the vertical structure and the spectra of the projected and full forecast error.

In particular, the vertical distribution of squared total energy and the spectral distribution of squared total energy (in terms of total wave number) are considered.

Ex1: total energy vertical distribution for Feb 1996 case

The top panel shows the vertical distribution of squared total energy for the pseudo-inverse field at initial (solid red) and final (solid blue) time. Dotted lines show the kinetic component.

The bottom panel shows the vertical distribution of squared total energy of the forecast error inside the area A, scaled by 0.2 compared to the top panel.

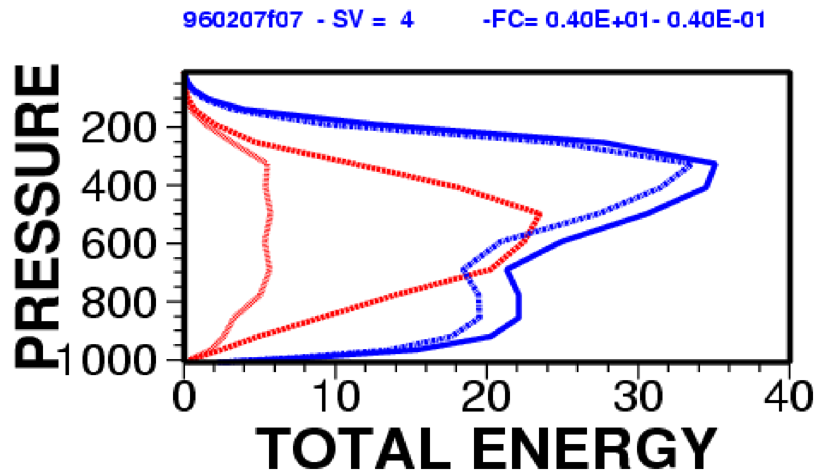

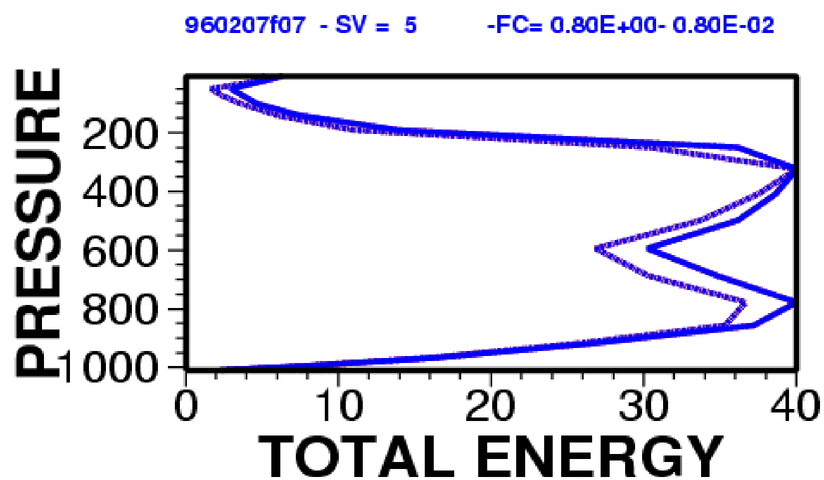

Ex1: total energy spectra for Feb 1996 case

The top panel shows the spectral distribution of squared total energy for the pseudo-inverse field at initial (solid red) and final (solid blue) time.

The bottom panel shows the vertical distribution of squared total energy of the forecast error inside the area A, scaled by 0.2 compared to the top panel.

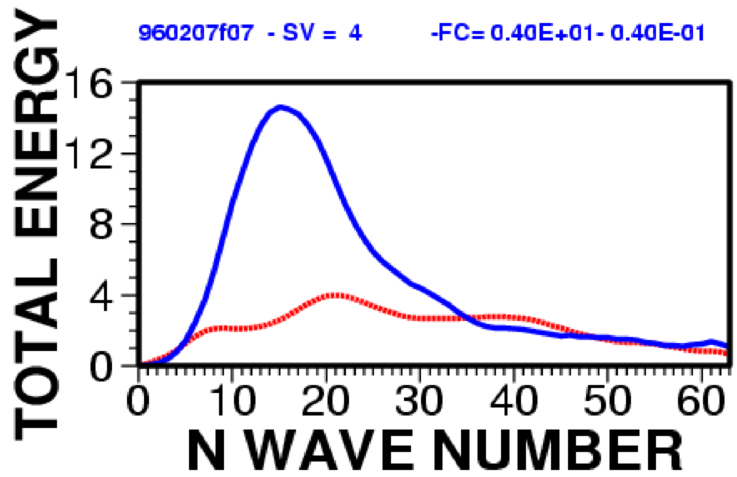

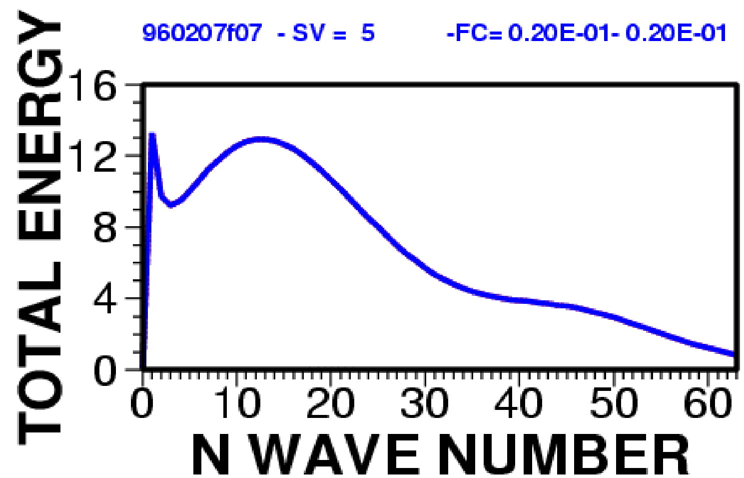

Ex2: total energy vertical distribution for Mar 1996 case

The top panel shows the vertical distribution of squared total energy for the pseudo-inverse field at initial (solid red) and final (solid blue) time. Dotted lines show the kinetic component.

The bottom panel shows the vertical distribution of squared total energy of the forecast error inside the area A, scaled by 0.2 compared to the top panel.

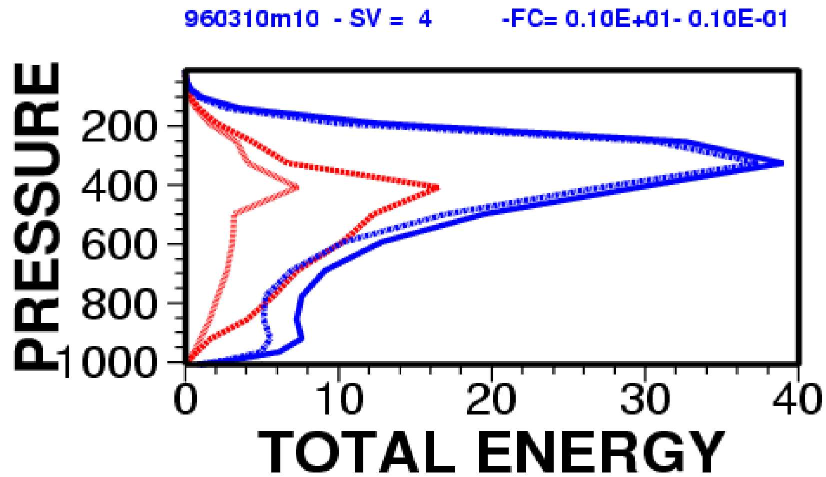

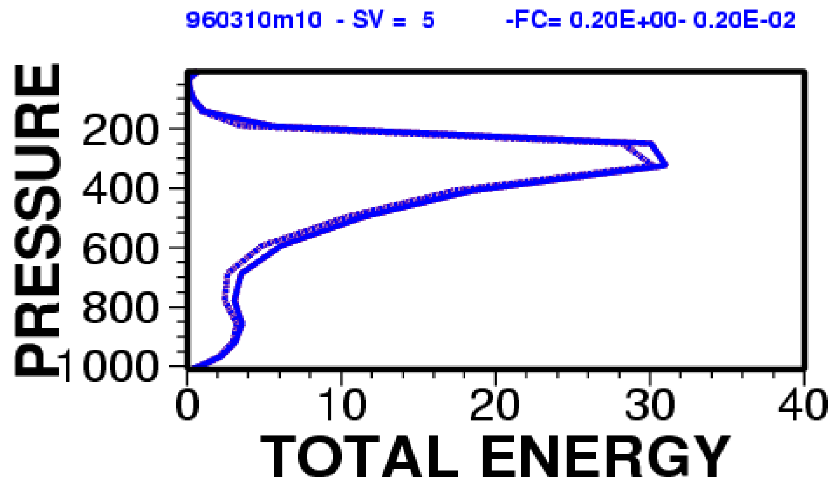

Ex2: total energy spectra for Mar 1996 case

The top panel shows the spectral distribution of squared total energy for the pseudo-inverse field at initial (solid red) and final (solid blue) time.

The bottom panel shows the vertical distribution of squared total energy of the forecast error inside the area A, scaled by 0.2 compared to the top panel.

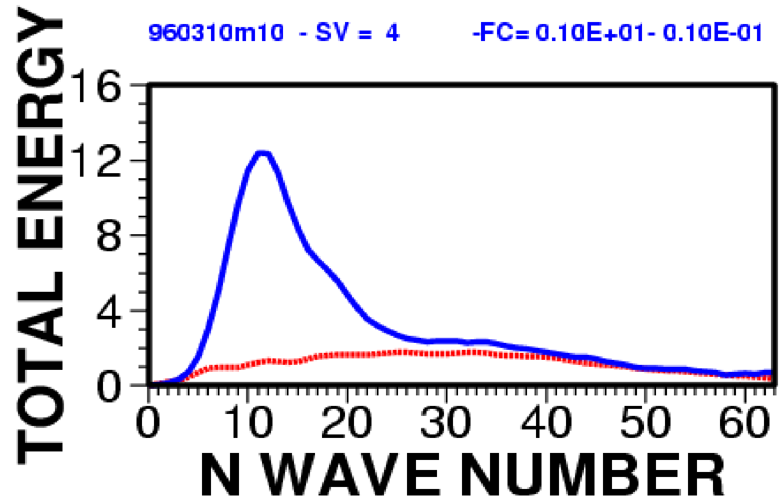

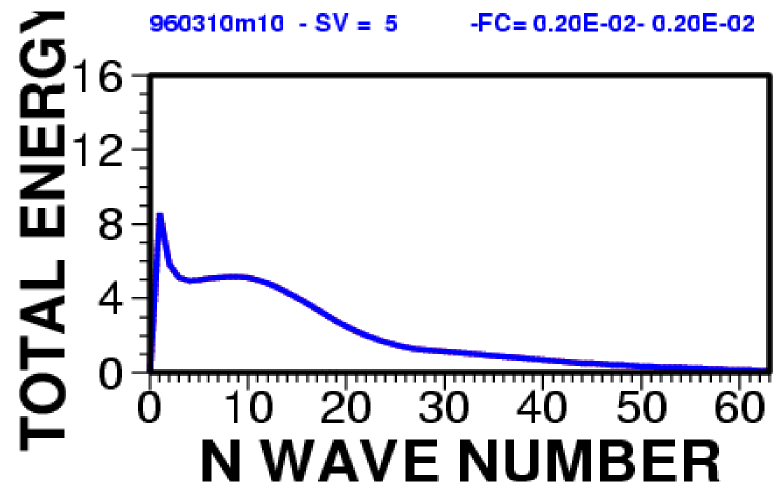

Considerations on total energy distributions and spectra

- Results confirm that the most of the forecast error inside the region A={40:60N;20-0W} is included in the sub-space of the phase-space of the system spanned by the leading 4 singular vectors.

- The initial time pseudo-inverse initial perturbation can be used to identify the geographical region where forecast error originated.

- The pseudo-inverse time evolution reflects the singular vector time evolution, with an upward and upscale energy propagation.

- At initial time, the pseudo-inverse total energy has a strong potential component, while at final time the pseudo-inverse total energy is dominated by the kinetic component.

Conclusions

❖ Singular vectors identify phase-space directions characterized by maximum growth (as measured by a matrix E) during a finite time interval (called the optimization time interval).

❖ Singular vectors can be used in diagnostic studies to identify regions of possible origin of forecast errors.

❖ The time evolution of forecast error and of the component of the forecast error in the sub-space spanned by the leading singular vectors have been compared. Results suggest that the singular vectors identify the most dynamically important directions of the phase space of the system.

Selected bibliography on SVs and pseudo-inverse

- Buizza, R., Tribbia, J., Molteni, F., & Palmer, T. N., 1993: **Computation of optimal unstable structures for a numerical weather prediction model**. *Tellus*, 45A, 388-407.
- Buizza, R., Gelaro, R., Molteni, F., & Palmer, T. N., 1997: **The impact of increased resolution on predictability studies with singular vectors**. *Q. J. R. Meteorol. Soc.*, 123, 1007-1033.
- Buizza, R., & Montani, A., 1999: **Targeting observations using singular vectors**. *J. Atmos. Sci.*, 56, 2965-2985.
- Cardinali, C., & Buizza, R., 2003: **Forecast skill of targeted observations: a singular-vector-based diagnostic**. *J. Atmos. Sci.*, 60, 1927-1940.
- Farrell, B. F., 1989: Optimal excitation of baroclinic waves. *J. Atmos. Sci.*, 46, 1193-1206.
- Gelaro, R., Buizza, R., Palmer, T. N., & Klinker, E., 1998: **Sensitivity analysis of forecast errors and the construction of optimal perturbations using singular vectors**. *J. Atmos. Sci.*, 55, 1012-1037.
- Golub, G. H., & van Loan, C. F., 1983. ***Matrix computation***. North Oxford Academic Publ. Co. LtD., Oxford, UK, 476pp.
- Lorenz, E., 1965: **A study of the predictability of a 28-variable atmospheric model**. *Tellus*, 17, 321-333
- Montani, A, Thorpe, A. J., Buizza, R., & Unden, P., 1999: **Forecast skill of the ECMWF model using targeted observations during FASTEX**. *Q. J. R. Meteorol. Soc.*, 125, 3219-3240.
- Palmer, T. N., Gelaro, R., Barkmeijer, J., & Buizza, R., 1998: **Singular vectors, metrics, and adaptive observations**. *J. Atmos. Sci.*, 55, 633-653.